# PAPER 4

Submitted for publication in *Journal of Materials Chemistry*

# Crystal structure, thermal and magnetic properties of $La_4Co_3O_9$. Phase relations for $La_4Co_3O_{10+\delta}$ ($-1.00 \leq \delta \leq 0.00$) at 673 K

Ole H. Hansteen[a], Helmer Fjellvåg[a] and Bjørn C. Hauback[b]

[a] *Department of Chemistry, University of Oslo, N-0315 Oslo, Norway*

[b] *Institutt for energiteknikk, N-2007 Kjeller, Norway*

---

## Abstract

Phase relations and reoxidation behaviour is reported for samples with nominal composition $La_4Co_3O_{10+\delta}$ ($-1.00 \leq \delta \leq 0.00$) synthesized by isothermal reduction at 673 K. The crystal structure of $La_4Co_3O_9$ has been determined on the basis of high resolution powder X-ray diffraction and neutron diffraction data. The space group is *Pnma*, $a$ = 545.716 (5) pm, $b$ = 2855.33 (3) pm, $c$ = 565.415 (5) pm; $R_{wp}$(PXD) = 6.2%, $R_{wp}$(PND) = 9.0%, $R_p$(PXD) = 4.4%, $R_p$(PND) = 7.0%. Reduction of $La_4Co_3O_{10}$ into $La_4Co_3O_9$ leads to ordering of oxygen vacancies. Chains of corner-sharing $CoO_4$-tetrahedra running along [100] are formed within the central-layer of each triple perovskite type layer of the Ruddlesden-Popper type structure of $La_4Co_3O_{10}$, whereas the top and bottom layers retain the perovskite type arrangement of corner-sharing $CoO_6$-octahedra. $La_4Co_3O_9$ orders antiferromagnetically at temperatures below $T_N$ = 303 ± 5 K. The magnetic structure is described on the basis of powder neutron diffraction data. The magnetic moments $\mu_{tetr.} = 2.6 \pm 0.1\mu_B$ and $\mu_{oct.} = 3.0 \pm 0.1\mu_B$ corresponds fairly well to spin only values for high-spin $Co^{II}$.

## Introduction

Low temperature reductions ($T$ < 900 K) of transition metal perovskite type oxides may proceed topotactically and lead to the formation of ordered oxygen deficient intermediate phases,[1] frequently with major changes in the physical properties. Such phases are connected with a lower valence state for the transition metal component. For example, two ordered intermediate phases are formed upon reduction of $LaCoO_3$, namely $La_3Co_3O_8$ and $La_2Co_2O_5$,[2, 3] where cobalt is (partly) reduced from the trivalent to the divalent state. The cationic sublattice of $LaCoO_3$ is essentially unchanged during the reductions, whereas ordering of oxygen vacancies leads to layers containing chains of corner-sharing $CoO_4$-tetrahedra connecting perovskite type layers of corner-sharing $CoO_6$-octahedra. The crystal structure of $La_2Co_2O_5$ is of the well known brownmillerite type.

$La_4Co_3O_{10}$ adopts the (layered) Ruddlesden-Popper type structure, belonging to the series $La_{m+1}Co_mO_{3m+1}$ with $m = 3$. The crystal structure consists of perovskite type triple-layers which are translated relatively to each other in the basal plane of the unit cell,[4] thereby breaking up the three dimensional network of corner-sharing $CoO_6$-octahedra of the perovskite structure. The octahedrally coordinated trivalent cobalt atoms in the perovskite layers suggests the possibility of forming oxygen deficient intermediate phases upon low temperature reduction of $La_4Co_3O_{10}$ analogous to the reduction described for $LaCoO_3$.

The present study focuses on phase relations for $La_4Co_3O_{10+\delta}$, $-1.00 \leq \delta \leq 0.00$, at 673 K. The crystal and magnetic structure of the ordered, reduced phase $La_4Co_3O_9$ has been determined on the basis of a combined analysis of high resolution powder X-ray diffraction data collected at ESRF and powder neutron diffraction data.

## Experimental

### Synthesis

Samples of nominal compositions $La_4Co_3O_{10+\delta}$ ($-1.00 \leq \delta \leq 0.00$) were prepared by isothermal reduction of single phase $La_4Co_3O_{10}$, which was first prepared by a citrate precursor method.[4] The starting materials for the synthesis of $La_4Co_3O_{10}$ were $La_2O_3$ (99.99% Molycorp), $Co(CH_3COO)_2{\cdot}4H_2O$ (>99% Fluka) and citric acid monohydrate, $C_3H_4(OH)(COOH)_3{\cdot}H_2O$ (>99.8% Riedel-de Haën). Single phase $La_4Co_3O_{10}$ was obtained after calcination of the precursor powder in nitrogen at 1300 K for 110 hours with two intermediate grindings followed by repelletization. Phase purity was assured from powder X-ray diffraction. The isothermal reduction of $La_4Co_3O_{10}$ was performed in sealed silica glass ampoules using chips of

Zr (99.5% a. D. Mackay Inc.) as reducing agent (oxygen getter). The ampoules, with the samples, were repeatedly flushed with argon before evacuation and sealing in order to minimize the amount of gaseous oxygen in the system prior to reduction. The sample was held in an alumina crucible at 673 K, and was separated (by approximately 160 mm) from the Zr, which was positioned in the warmer zone of the furnace at 873 K in order to assure complete oxidation to $ZrO_2$.[2] After reaction and equilibration for seven days, all samples were cooled in ice-water. The ampoules were opened in an argon filled glovebox [$p(O_2)$ and $p(H_2O) < 1$ ppm]. Care was taken to assure inert atmosphere during storage, handling and subsequent characterization of specimens.

**Powder diffraction**

Room temperature powder X-ray diffraction (PXD) data were collected for all samples with a Guinier Hägg camera using Si as internal standard ($a$ = 543.1065 pm). The sample holders were filled with oil and sealed with Scotch tape on top and bottom. The sample adhered to the bottom tape which prevented it from dispersing into the oil. Both Cr$K\alpha_1$ (detection limit for impurities ca. 0.3 wt%)[5] and Cu$K\alpha_1$ radiation were used. The programs TREOR [6] and UNITCELL [7] were used for unit cell indexing and least squares determination of unit cell dimensions. Synchrotron (SR) PXD data were collected for $La_4Co_3O_9$ with the powder diffractometer in Debye-Scherrer mode at the Swiss Norwegian Beam Line (BM1) at ESRF (Grenoble). Monochromatic X-rays of wavelength 110.103 pm were obtained from a channel-cut Si(111) crystal. The sample was contained in a sealed and rotating glass capillary with diameter 0.5 mm. Intensity data were collected at 298 K between $2\theta$ = 8 and 70° in steps of $\Delta(2\theta)$ = 0.007°. Powder neutron diffraction (PND) data were collected for $La_4Co_3O_9$ with the two-axis powder diffractometer PUS at the JEEP II reactor, Kjeller (Norway). A cylindrical sample holder of vanadium, carefully sealed with an indium washer, was used. Monochromatized neutrons of wavelength 153.79 pm were obtained by reflection from Ge(511) of the focusing composite germanium monochromator. The scattered intensities were measured by two detector units. Each detector unit contains a vertical stack of seven position sensitive $^3$He detectors which covers 20° in $2\theta$. Intensity data were collected at 10 K and 298 K between $2\theta$ = 10 and 130°. The steplength between data points was $\Delta(2\theta)$ = 0.05°. The GSAS program package[8] was used for combined Rietveld-type profile refinements of powder synchrotron X-ray and neutron diffraction data collected at 298 K. Table 1 summarizes characteristic features of the data sets and the variable parameters entering the least-squares

**Table 1** Characteristic features of the powder synchrotron X-ray (298 K) and neutron diffraction (10, 298 K) data sets for $La_4Co_3O_9$, and list of parameters entering into the Rietveld type refinements.

| | PXD(SR) | | PND | |
|---|---|---|---|---|
| Measured data points | 8857 | | 2398 | |
| Reflections (hkl) | 544 | | 790 | |
| $\lambda$ (pm) | 110.103 | | 153.79 | |
| Scale factor | 1 | | 1 | |
| Zero point | 1 | | 1 | |
| Profile parameters | 6 | | 3 | |
| Unit cell dimensions | | 3[a] | | |
| Positional parameters | | 25[a] | | |
| Isotropic displacement factors | | 3[a] | | |
| Magnetic vector components | | | (2)[b] | |
| Background coefficients | 6 | | 15 | |
| Refinable parameters | 14 + | 31 + | 20 | = 65 |

[a] Common parameters for PXD(SR) and PND in the combined refinements.
[b] Only refined for the 10 K data.

refinements. The background was modelled by cosine Fourier series polynomials for both datasets. The peak shape of the synchrotron diffraction pattern was modelled by a pseudo-Voigt function using three Gaussian half width parameters (U, V, W) and two Lorentzian coefficients (one Scherrer broadening coefficient and one strain broadening coefficient). For the PND data, the peak shape was modelled by a Gaussian function. The scattering lengths $b_{La}$ = 8.27 fm, $b_{Co}$ = 2.53 fm and $b_O$ = 5.81 fm were taken from the GSAS library. For profile refinement of the PND data collected at 10 K (crystal and magnetic structure) the Hewat version[9] of the Rietveld program[10] was used.

High temperature PXD data were collected upon continuous heating using a Guinier Simon camera (Enraf Nonius) and Cu$K\alpha_1$ radiation. The sample was kept in a rotating silica-glass capillary. Photographic film was used as detector and the temperature change was synchronized with the movement of the film cassette. The temperature was calibrated by means of measurement of the thermal expansion of silver.[11]

**Thermal analysis**

Thermogravimetric (TGA) analysis was performed with a Perkin Elmer TGA7. Data reduction was performed with standard programs for the systems.

### Magnetic measurements

Magnetic susceptibility data were measured by a Quantum Design SQUID-magnetometer (MPMS) in the temperature range 2 - 300 K with magnetic fields ($H$) up to 50.0 kOe. All samples were zero field cooled and the temperature dependence of the magnetic susceptibility was measured on heating. The samples were held in evacuated and sealed spherical silica glass ampoules. The measured magnetic susceptibility was corrected for diamagnetic contributions from the sample container and from core electrons.

## Results and Discussion

### Phase relations for $La_4Co_3O_{10+\delta}$, $-1.00 \leq \delta \leq 0.00$

Samples were synthesized with nominal compositions $La_4Co_3O_{10+\delta}$, $-1.00 \leq \delta \leq 0.00$. The compositions $\delta = -0.50$ and $\delta = -1.00$ correspond respectively to the reduction of half (one) and all (two) of the trivalent cobalt atoms in $La_4Co_3O_{10}$. According to PXD at 298 K only two distinct phases occur for $-1.00 \leq \delta \leq 0.00$, namely $La_4Co_3O_{10}$ ($\delta = 0.00$) and $La_4Co_3O_9$ ($\delta = -1.00$). The samples with other nominal compositions, including those with only minor deviation from the stoichiometric compositions $\delta = 0.00$ and $-1.00$, were identified as two phase mixtures, thereby excluding any larger non-stoichiometry for these phases under the present conditions.

The direct phase conversion of $La_4Co_3O_9$ into $La_4Co_3O_{10}$ was verified by oxidation in air using high temperature PXD and TGA. Figure 1 shows, schematically, the changes in the high temperature PXD pattern of $La_4Co_3O_9$ upon oxidation. The sample was subjected to air immediately before starting the experiment. The single phase regimes for $La_4Co_3O_9$ and $La_4Co_3O_{10}$ are separated by a reaction regime at around 320 K where the two phases coexist (shaded background). Figure 2 shows the weight change upon oxidation of $La_4Co_3O_9$ using TGA. The oxidation rate changes at 400 K after an initial 1% weight increase, which approximately corresponds to $\delta = -0.5$. The weight shows a maximum at approximately 600 K corresponding to the composition $La_4Co_3O_{10.18}$. The maximum is characteristic for the oxidative non-stoichiometry ($\delta > 0.00$) of $La_4Co_3O_{10+\delta}$ when heated in air.[4] PXD of samples oxidized at temperatures below 1250 K verify complete oxidation of $La_4Co_3O_9$ into $La_4Co_3O_{10+\delta}$ ($\delta > 0.00$). The second weight increase starting above 1250 K corresponds to oxidation of $La_4Co_3O_{10+\delta}$ into a two phase mixture of $LaCoO_3$ and $La_2O_3$.

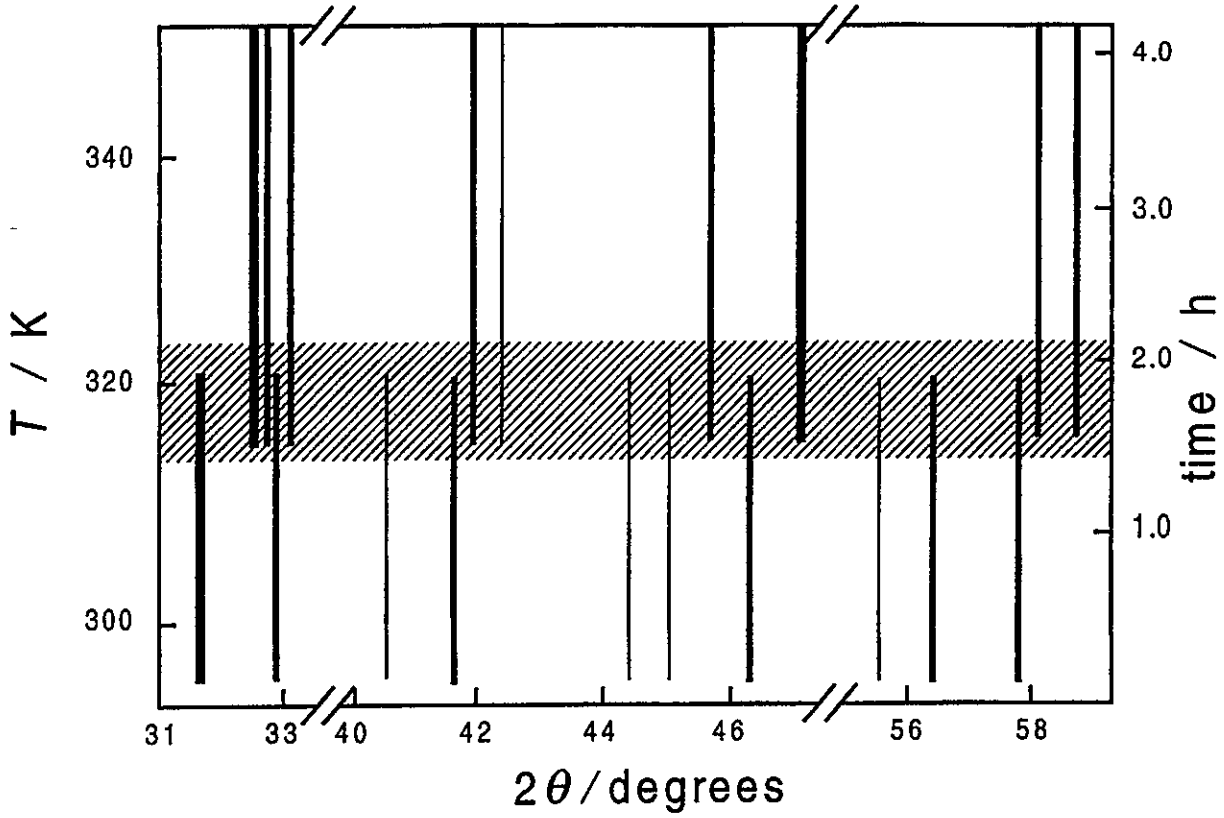


**Fig. 1** Schematic representation of parts of the high temperature PXD pattern during oxidation of $La_4Co_3O_9$ in air. Heating rate 0.23 K $min^{-1}$, $\lambda = 154.0598$ pm.

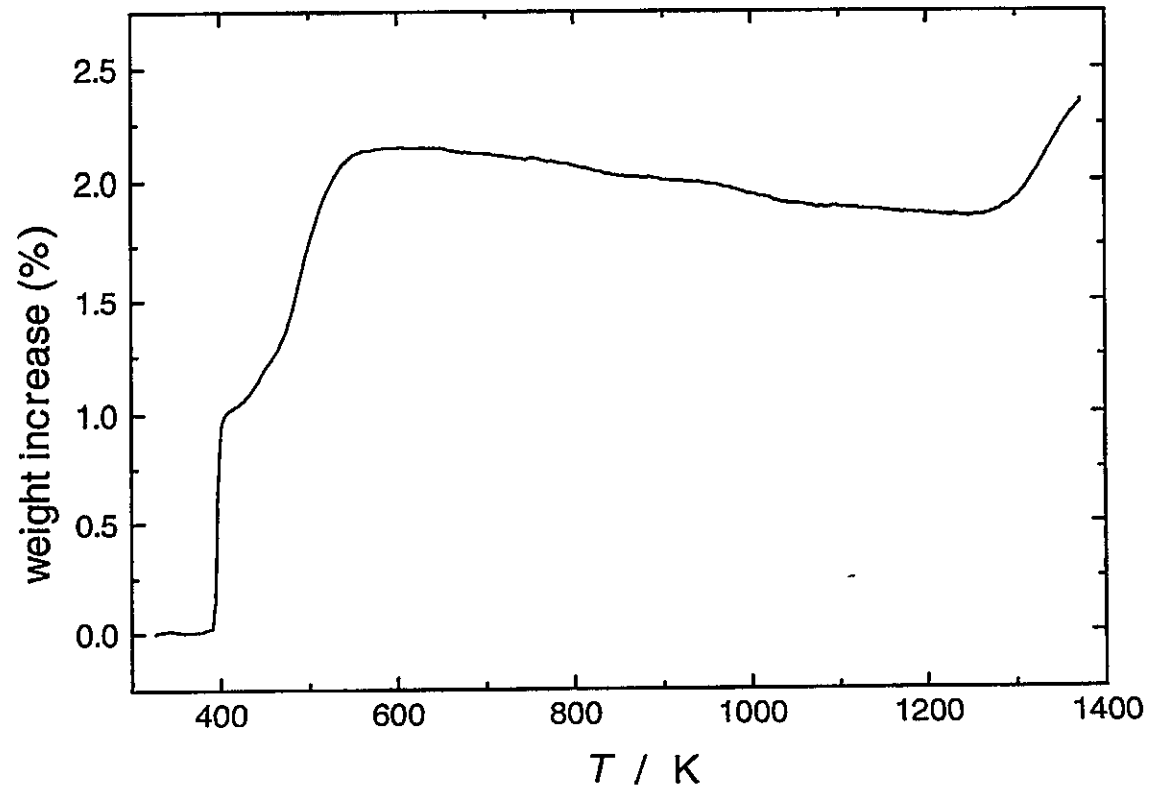


**Fig. 2** Thermogravimetric data for oxidation of $La_4Co_3O_9$ in air. Heating rate 5 K $min^{-1}$.

**Crystal structure of $La_4Co_3O_9$**

All reflections in the Guinier-Hägg PXD patterns at 298 K for $La_4Co_3O_9$ could be satisfactorily indexed on a primitive orthorhombic unit cell; $a$ = 545.2 (1) pm, $b$ = 2852.1 (6) pm, $c$ = 565.5 (1) pm. The unit cell volume is expanded by 6.9 % relative to the unit cell of $La_4Co_3O_{10}$ [space group *C2/m*, $a$ = 541.79 (1) pm, $b$ = 547.56 (1) pm, $c$ = 2780.5 (1) pm, $\beta$ = 90.200 (1) °][4] and is most prominent along $\bar{b}$ and $\bar{c}$. The volume expansion is mainly caused by the reduction of $Co^{III}$($d^6$, low-spin) to the larger sized $Co^{II}$($d^7$). The initial structure model for the profile refinements was based on the Ruddlesden-Popper atomic arrangement for $La_4Co_3O_{10}$ [4] modified by introducing ordered oxygen vacancies in analogy to the reduced phases of $LaCoO_3$, namely $La_3Co_3O_8$ and $La_2Co_2O_5$.[2, 3] It was assumed that *i*) the cationic sublattice is essentially unchanged, *ii*) the oxygen vacancies are ordered within the triple perovskite layers, resulting in chains of $CoO_4$-tetrahedra parallel to the shortest unit cell axis, and *iii*) the displacements of the oxygen atoms and the tetrahedrally coordinated cobalt atoms are similar to those found for $La_3Co_3O_8$ and $La_2Co_2O_5$. Considering the well defined peaks in the synchrotron PXD and the PND profiles three possible space groups were indicated, *Pnma*, $Cmc2_1$ or $C222_1$. However, a close inspection of the diffraction profiles revealed intensity slightly above the background signal for several reflections; (*hk*0) for $k = 2n+1$, (*h*0*l*) for $l = 2n+1$ and (*hkl*) for $k+l = 2n+1$, which should be absent for the space groups $Cmc2_1$ and $C222_1$. Hence, the centro-symmetric space group *Pnma* was adopted. The refinements converged satisfactorily and the results of the combined Rietveld refinements of the synchrotron PXD and the PND data are given in Tables 2 - 4. Observed, calculated and difference intensity profiles are shown in Fig. 3.

The crystal structure of $La_4Co_3O_9$ is shown in Fig. 4. The unit cell comprises two triple-layers for which the cationic sublattice of $La_4Co_3O_{10}$ is to a large degree preserved during the reduction. Ordering of oxygen vacancies lead to chains of corner-sharing $CoO_4$-tetrahedra parallel to [100] within the central part of each perovskite type triple-layer. The top and bottom part of each triple-layer retain the perovskite type arrangement of corner-sharing $CoO_6$-octahedra. Co(1) and the oxygen atoms are somewhat displaced relative to the atomic positions for $La_4Co_3O_{10}$. Just as for the reduced phase $La_2Co_2O_5$,[3] these displacements and the expansion of $\bar{c}$ reduce the distortions of the $CoO_4$-tetrahedra and considerable tilting of the $CoO_6$-octahedra occurs. Despite the atomic displacements there are still considerable distortions of the tetrahedra especially along [010] as shown by the large O(5)—Co(1)—O(5) angle and short Co(1)—O(5) interatomic distances (Table 4). Furthermore, the $CoO_6$-

octahedra are significantly elongated along [010], and the nine fold coordination of oxygen around lanthanum is irregular.

**Table 2** Unit cell data for $La_4Co_3O_9$ and reliability factors. Calculated standard deviations in parentheses.

| | | 298 K | 10 K |
|---|---|---|---|
| Crystal system | | Orthorhombic | Orthorhombic |
| Space group | | *Pnma* | *Pnma* |
| *a*, pm | | 545.716 (5) | 543.56 (2) |
| *b*, pm | | 2855.33 (3) | 2846.0 (1) |
| *c*, pm | | 565.415 (5) | 564.67 (2) |
| *V*, $10^8$pm$^3$ | | 8.8103 (2) | 8.7352 (7) |
| *Z* | | 4 | 4 |
| $R_p$ (%) [a] | PXD | 4.4 | |
| | PND | 7.0 | 9.8[b] |
| $R_{wp}$ (%) [a] | PXD | 6.2 | |
| | PND | 9.0 | 16.1 |
| $R_{exp}$ (%) | PXD | 2.9 | |
| | PND | 4.2 | 10.0 |
| $\chi^2$ | | 4.50 | 2.60 |

[a] $R_p = 100(\Sigma|I_O-I_C|/\Sigma I_O)$ , $R_{wp} = 100(\Sigma w(I_O-I_C)^2/\Sigma w I_O^2)^{-1/2}$ according to Ref. 8 (298 K) and Refs. 9, 10 (10 K). [b] Combined refinement, crystallographic ($R_N = 9.7\%$) and magnetic ($R_M = 10.6\%$).

**Table 3** Fractional atomic coordinates for $La_4Co_3O_9$ at 298 K. Calculated standard deviations in parentheses. Space group *Pnma*. Isotropic displacement factors ($B_{iso}$ in $10^4$pm$^2$): $B_{iso}$(La) = 1.92 (5), $B_{iso}$(Co) = 1.02 (1), $B_{iso}$(O) = 0.87 (8).

| Atom | Wückoff site[a] | Coordinates | | |
|---|---|---|---|---|
| | | *x* | *y* | *z* |
| La(1) | *8d* | 0.250 (1) | 0.0492 (1) | 0.9863 (6) |
| La(2) | *8d* | 0.248 (1) | 0.1724 (1) | 0.0157 (6) |
| Co(1) | *4c* | 0.212 (2) | 0.25 | 0.551 (1) |
| Co(2) | *8d* | 0.251 (3) | 0.1100 (2) | 0.500 (2) |
| O(1) | *4c* | 0.353 (3) | 0.25 | 0.889 (2) |
| O(2) | *8d* | 0.260 (4) | 0.0300 (3) | 0.555 (2) |
| O(3) | *8d* | 0.995 (5) | 0.1045 (3) | 0.245 (4) |
| O(4) | *8d* | 0.997 (5) | 0.1194 (3) | 0.758 (4) |
| O(5) | *8d* | 0.248 (4) | 0.1877 (3) | 0.431 (1) |

[a] *4c* (*x*,¼,*z*), *8d* (*x*,*y*,*z*)

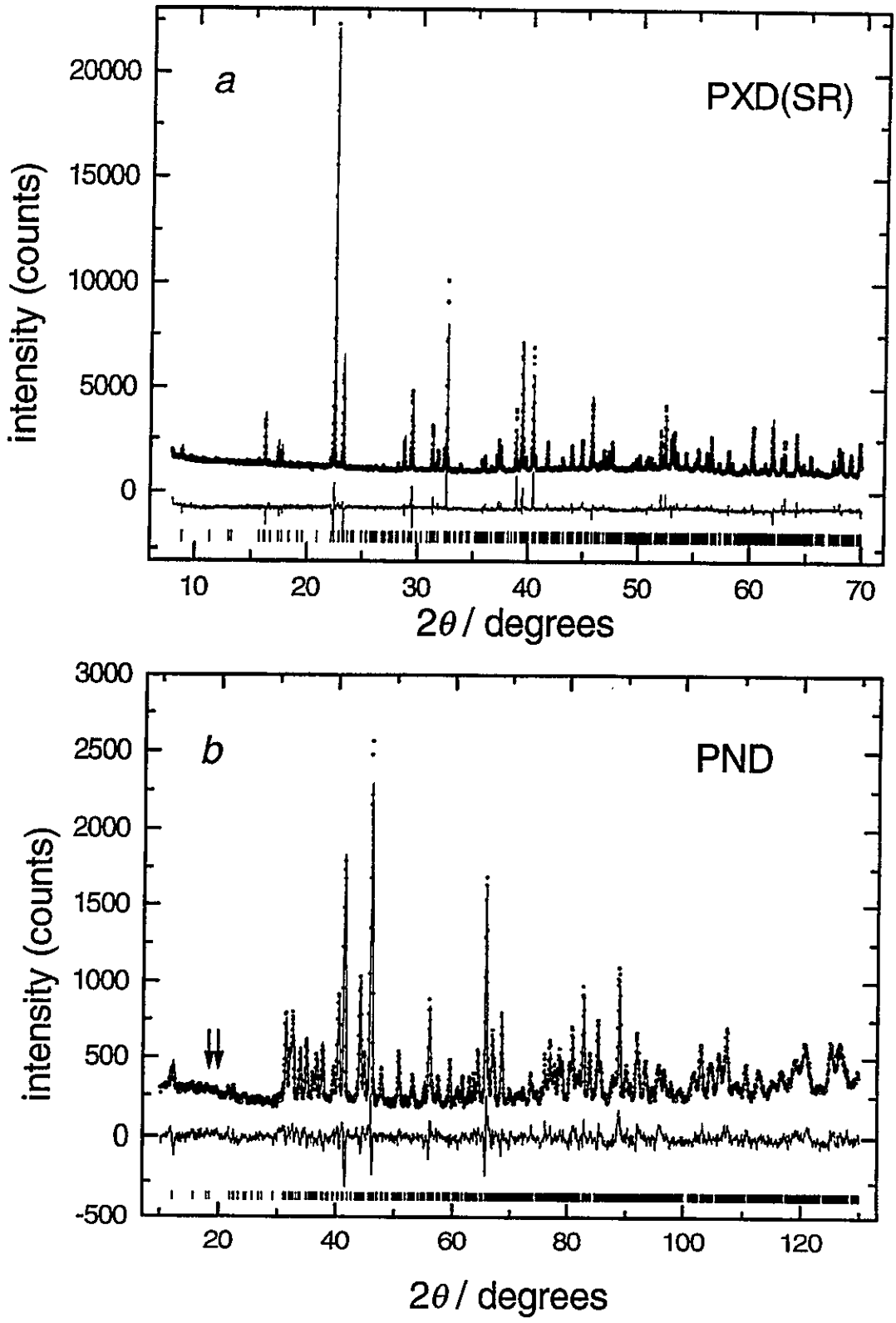


**Fig. 3** a) Synchrotron PXD ($\lambda$ = 110.103 pm) and b) PND ($\lambda$ = 153.79 pm) profiles for $La_4Co_3O_9$ at 298 K. Experimental points marked by open circles, calculated profile by full line; lower full line marks difference plot, vertical bars marks positions for Bragg reflections.

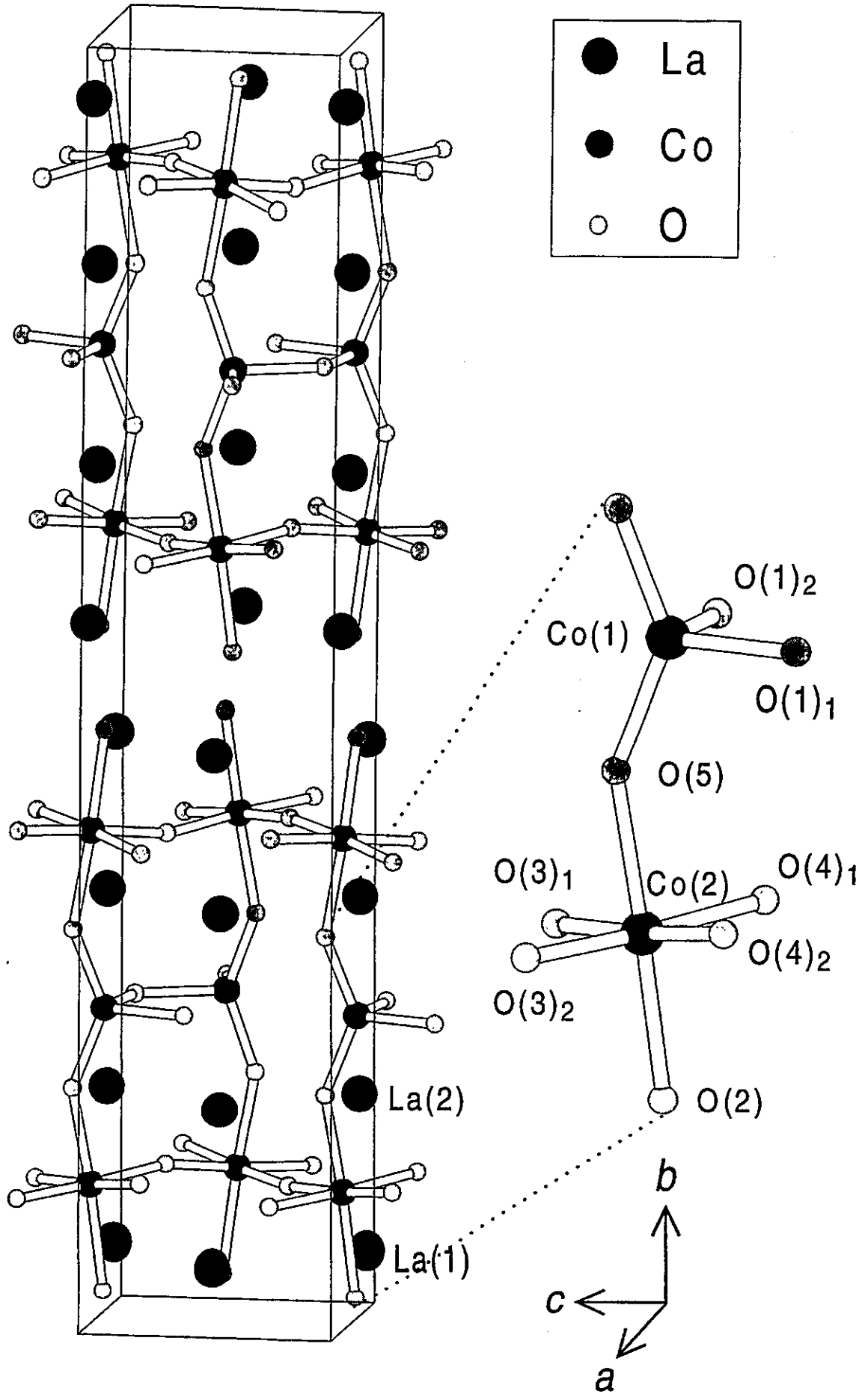


Fig. 4 Crystal structure for $La_2Co_2O_5$. Space group *Pnma*.

**Table 4** Selected interatomic distances and bond angles for $La_4Co_3O_9$ at 298 K. Calculated standard deviations in parentheses. Atom numbers refer to Fig. 4.

| | Distances (pm) | | | Angles (°) | |
|---|---|---|---|---|---|
| Tetrahedron: | Co(1) — $O(1)_1$ | | 206 (1) | $O(1)_1$—Co(1)—$O(1)_2$ | 102.3 (1) |
| | — $O(1)_2$ | | 198 (1) | $O(1)_1$—Co(1)—O(5) | 106.9 (1) |
| | — O(5) | (×2) | 191 (1) | $O(1)_2$—Co(1)—O(5) | 99.3 (1) |
| | | | | O(5)—Co(1)—O(5) | 136.5 (1) |
| Octahedron: | Co(2) — O(2) | | 230 (1) | O(2)—Co(2)— $O(3)_1$ | 92.0 (1) |
| | — $O(3)_1$ | | 201 (1) | O(2)—Co(2)— $O(3)_2$ | 90.0 (1) |
| | — $O(3)_2$ | | 193 (1) | O(2)—Co(2)— $O(4)_1$ | 92.9 (1) |
| | — $O(4)_1$ | | 201 (1) | O(2)—Co(2)— $O(4)_2$ | 91.5 (1) |
| | — $O(4)_2$ | | 193 (1) | O(5)—Co(2)— $O(3)_1$ | 86.9 (1) |
| | — O(5) | | 225 (1) | O(5)—Co(2)— $O(3)_2$ | 87.7 (1) |
| | | | | O(5)—Co(2)— $O(4)_1$ | 89.4 (1) |
| | | | | O(5)—Co(2)— $O(4)_2$ | 89.5 (1) |
| | | | | $O(4)_1$—Co(2)— $O(4)_2$ | 87.1 (1) |
| | | | | $O(3)_1$—Co(2)— $O(3)_2$ | 87.5 (1) |
| | | | | $O(3)_1$—Co(2)— $O(4)_1$ | 93.0 (1) |
| | | | | $O(3)_2$—Co(2)— $O(4)_2$ | 92.2 (1) |

| | Distances (pm) | | Coordination |
|---|---|---|---|
| La(1) — O | 230 - 284, 326 (1) | 8 + 1 |
| La(2) — O | 239 - 278, 333 (1) | 8 + 1 |

| | | |
|---|---|---|
| Polyhedra tilt angles (°): | Co(1)—O(5)—Co(2) | 148.6 (1) |
| | Co(1)—O(1)—Co(1) | 121.8 (1) |
| | Co(2)—O(3)—Co(2) | 170.9 (1) |
| | Co(2)—O(4)—Co(2) | 164.4 (1) |

The low temperature reduction of $La_4Co_3O_{10}$ leads to structural changes completely analogous to those accompanying the reduction of $LaCoO_3$ via $La_3Co_3O_8$ to $La_2Co_2O_5$. The triple-layers in the unit cell of $La_4Co_3O_9$ are separated by layers with NaCl-type arrangement of La- and O-atoms. Hence, for emphasizing such structural building units the chemical formula of $La_4Co_3O_9$ can be rewritten as $LaO(La_3Co_3O_8)$. Similarly $La_4Co_3O_{10}$ can be rewritten as $LaO(LaCoO_3)_3$.

**Magnetic properties of $La_4Co_3O_9$**

The PND data for $La_4Co_3O_9$ at 10 K showed a number of additional reflections of magnetic origin, see Fig. 5. Their intensities gradually decrease on increasing temperature, with a more pronounced drop above 280 K (Fig. 6). There are still minor magnetic scattering at 298 K, slightly above the background level, for the reflections (031) and (140), cf. arrows in Fig. 3b. The antiferromagnetic ordering temperature $T_N = 303 \pm 5$ K is estimated by extrapolation of the integrated intensity for (031) to the background level (Fig. 6). All additional magnetic reflections (Fig. 5) could be indexed on the crystallographic unit cell. The cobalt atoms in the tetrahedra and octahedra are all divalent. All $Co^{II}$—O—$Co^{II}$ interactions were assumed to be antiferromagnetic in nature. A model of the magnetic structure based on antiferromagnetic ordering of the magnetic moments of all cobalt atoms is proposed. Successive triple layers with G-type ordering arrange as shown in Fig. 7. The refinements gave a reasonable fit to the experimental data, see Fig. 5, with magnetic $R$-factor $R_M = 10.6$ %. The refined magnetic moments were $\mu_{tetr} = 2.6 \pm 0.1\ \mu_B$ for Co(1) and $\mu_{oct} = 3.0 \pm 0.1\ \mu_B$ for Co(2), both moments

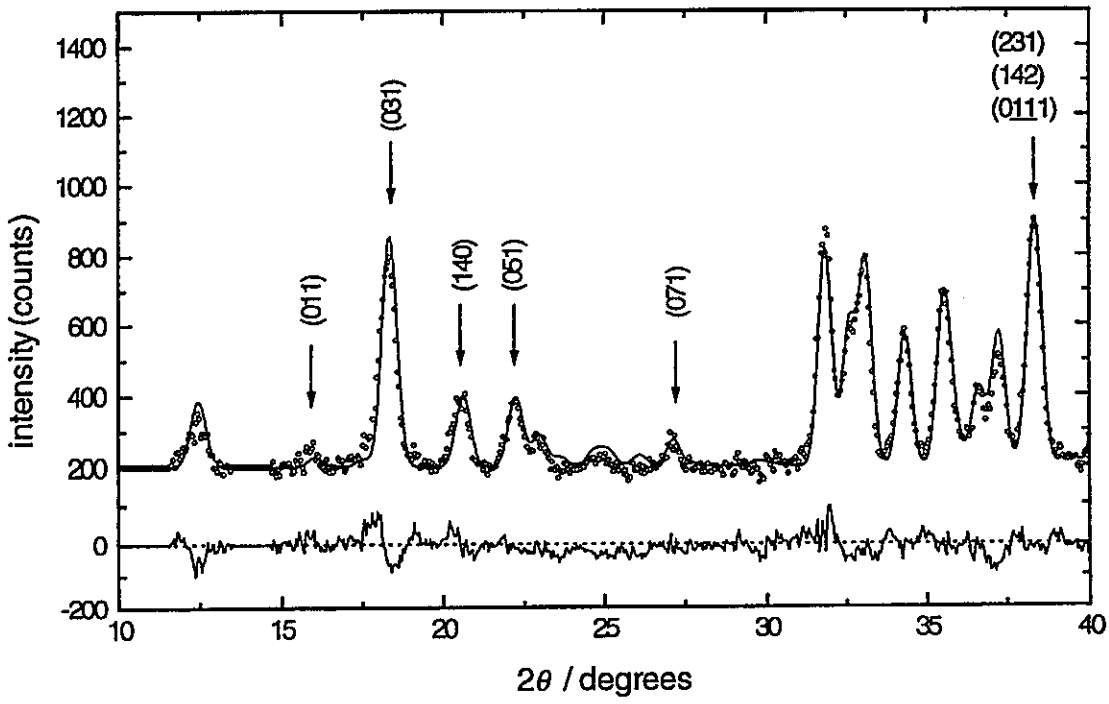


**Fig. 5** Selected parts of the PND profile for $La_4Co_3O_9$ at 10 K. Magnetic reflections are marked by arrows and Miller indices are given. Experimental points marked by open circles, full line marks calculated profile, and lower full line marks difference plot. Wavelength $\lambda =$ 153.79 pm.

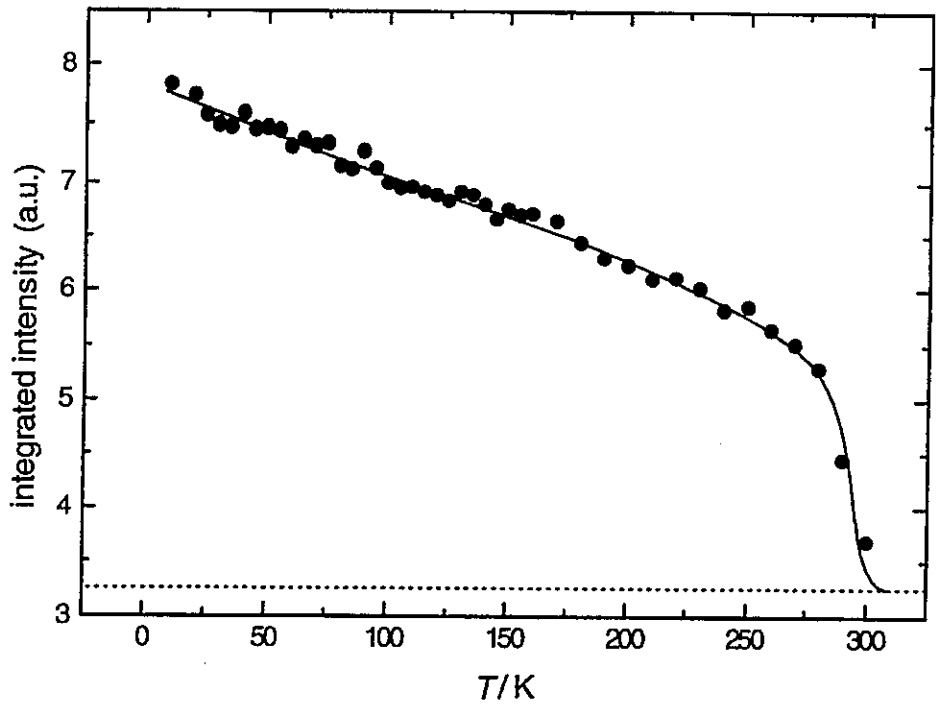


**Fig. 6** Temperature dependence of the integrated intensity for the magnetic PND reflection (031). Dashed line represents the background level. Fully drawn line as guide to the eye.

oriented parallel to [100]. The magnetic moment values correspond fairly well to that of $Co^{II}$ in the high-spin state ($S$ = 3/2). The derived magnetic moments for $La_4Co_3O_9$ correspond very well to those obtained for antiferromagnetic $La_2Co_2O_5$ (G-type ordering) with $T_N = 301 \pm 5$ K.[3] The magnetic coupling between successive triple perovskite layers in $La_4Co_3O_9$ is similar to that between single perovskite layers in $La_2CoO_4$. Note, $La_2CoO_4$ is the $Co^{II}$-representative of the Ruddlesden-Popper series $La_{m+1}Co_mO_{3m+1}$ with $m$ = 1.[12] In $La_2CoO_4$ antiferromagnetic ordering occurs within the single perovskite layer of octahedrally coordinated $Co^{II}$; magnetic moment $\mu_{oct} = 2.9 \pm 0.1\ \mu_B$, $T_N = 275$ K. Thus, for the three ternary phases of divalent cobalt in the La-Co-O system, $La_2CoO_4$, $La_2Co_2O_5$ and $La_4Co_3O_9$, strong antiferromagnetic coupling is present. This feature is typical for high spin $Co^{II}$ in oxides.

A small field hysteresis is observed for the magnetization, $M_g(H)$, at 298 K (see inset Fig. 8). Since $La_4Co_3O_9$ is antiferromagnetically ordered, it was concluded that the hysteresis most probably is caused by a minor ferromagnetic impurity of metallic cobalt not detectable by

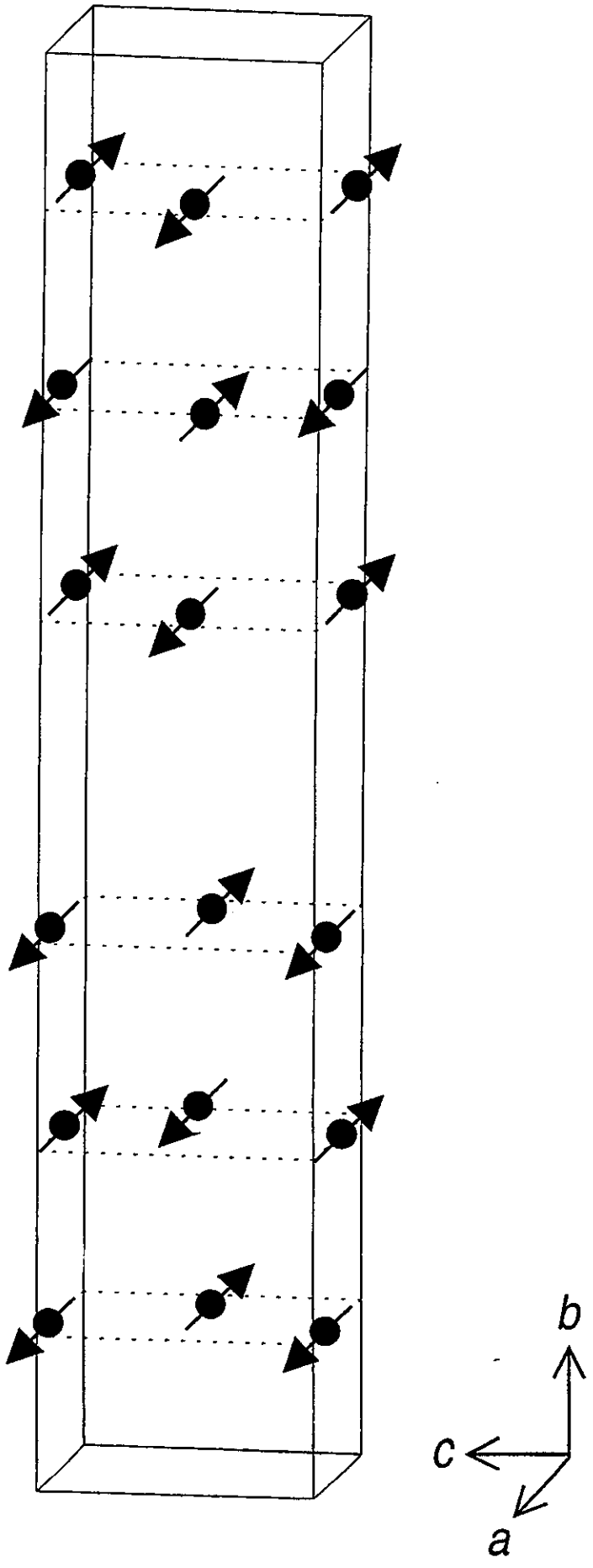


Fig. 7 Antiferromagnetic order in $La_2Co_2O_5$. Only Co-atoms shown.

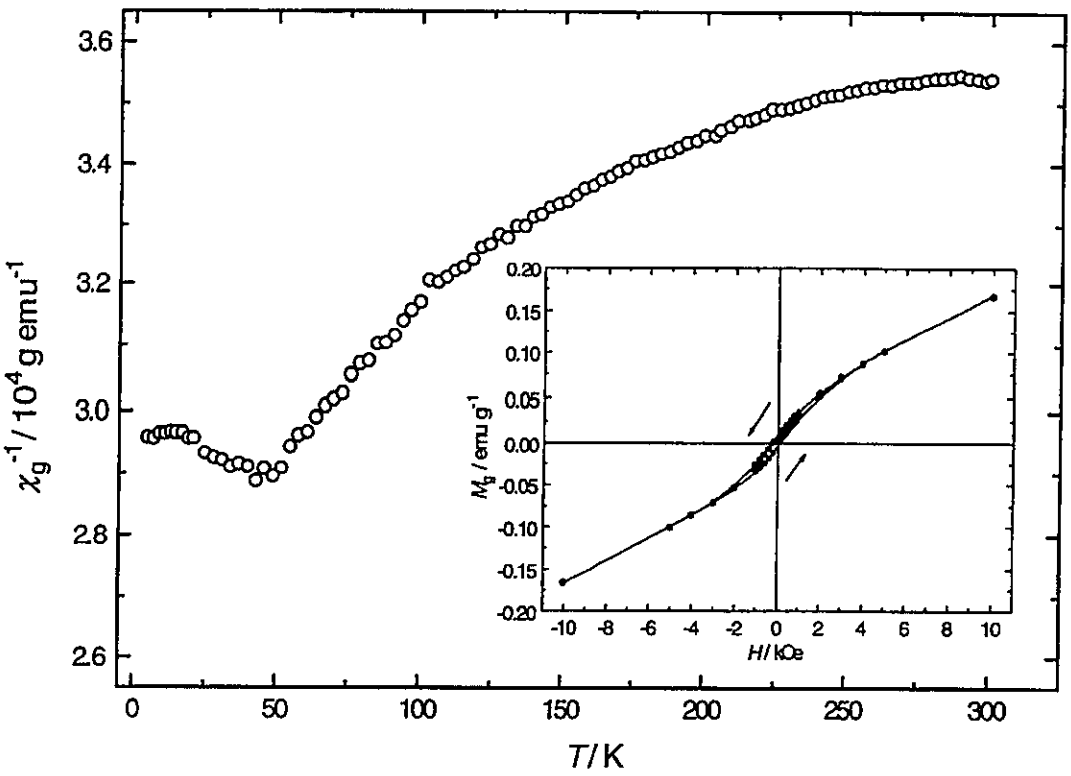


**Fig. 8** Temperature dependence of the inverse magnetic susceptibility ($\chi_g^{-1}$) for $La_4Co_3O_9$, measuring field $H = 200$ Oe. Inset shows field dependence of the magnetization ($M_g$) at 300 K.

PXD. Co(s) may be formed by e.g. enhanced surface reduction due to insufficient material equilibration (i.e. oxygen diffusion) under the adopted reduction conditions. Other possible causes are a small excess of reducing agent or reduction of minor amounts of cobalt oxide (CoO or $Co_3O_4$) impurities not detectable by PXD. Similar indications for minor ferromagnetic impurities of cobalt were found for $La_2Co_2O_5$.[3] The magnetic susceptibility, $\chi_g(T)$, of $La_4Co_3O_9$ decreases gradually with temperature for $T > 50$ K, but deviates significantly from Curie-Weiss behavior, Fig. 8. The cusp in $\chi_g(T)$ around 50 K could stem from a change in the antiferromagnetic ordering. However, no changes were observed for the integrated intensity of the magnetic PND reflections (Fig. 6). It is, however, likely that the $\chi_g(T)$ curve to a large extent reflects the properties of precipitated Co-particles. Depending on the particle size, they will show ferro- or superparamagnetic behaviour. The cusp at 50 K is possibly related to blocking of superparamagnetic particles.

**Acknowledgement**

This work has received financial support from the Research Council of Norway. The skilful assistance from project team at the Swiss-Norwegian Beam Line, ESRF is gratefully acknowledged. Contribution No 98.xx from the Swiss-Norwegian Beam Line at ESRF.

**References**

1 C. N. R. Rao, J. Gopalakrishnan and K. Vidyasagar, *Indian J. Chem. A*, 1984, **23**, 265

2 O. H. Hansteen, H. Fjellvåg and B. C. Hauback, *J. Mater. Chem.* submitted (Paper 1 of this thesis)

3 O. H. Hansteen, H. Fjellvåg and B. C. Hauback, *J. Solid State Chem.* submitted (Paper 2 of this thesis)

4 O. H. Hansteen and H. Fjellvåg, *J. Solid State Chem.* submitted (Paper 3 of this thesis)

5 B. Gilbu, H. Fjellvåg and A. Kjekshus, *Acta Chem. Scand.*, 1994, **48,** 37

6 P. E. Werner, L. Eriksson and M. Westdahl, *Program TREOR (version 5), J. Appl. Crystallogr.*, 1985, **18,** 367

7 B. Noläng, *Program UNITCELL,* Department of Chemistry, Uppsala University, Sweden

8 A. C. Larson and R. B. Von Dreele, *GSAS General Structure Analysis System,* LANSCE, MS-H 805, Los Alamos National Laboratory, Los Alamos, NM 87545, USA

9 A. W. Hewat, Harwell Report RRL 73/239, 1973

10 H. M. Rietveld, *J. Appl. Crystallogr.*, 1969, **2,** 65

11 J. Spreadborough and J. W. Christian, *J. Sci. Instrum.*, 1959, **36,** 116

12 K. Yamada, M. Matsuda, Y. Endoh, B. Keimer, R. J. Birgeneau, S. Onodera, J. Mizusaki, T. Matsuura and G. Shirane, *Phys. Rev. B*, 1989, **39,** 2336